

Effect of temperature on moisture absorption in a bismaleimide resin and its carbon fiber composites

Li-Rong Bao*, Albert F. Yee

Macromolecular Science and Engineering, University of Michigan, 3062 H.H. Dow Building, Ann Arbor, MI 48109, USA

Received 6 December 2001; received in revised form 21 February 2002; accepted 25 February 2002

Abstract

The effect of temperature on moisture absorption and hygrothermal aging in a commercial bismaleimide (BMI) resin and its composites are studied. The resin and composites display a two-stage diffusion behavior, with the first and second stages being diffusion- and relaxation-controlled, respectively. An increase in temperature accelerates moisture absorption in both the first and second stages. The activation energy of diffusion is very similar in the neat resin and composites, which suggests minimal interface effect on short term moisture diffusion. The equilibrium uptake of the diffusion-controlled first stage decreases with increasing temperature, indicating moisture absorption in the BMI resin is exothermic. The heat of absorption calculated from the temperature dependence of the quasi-equilibrium uptake is on the order of -3 kJ/mol. Although moisture absorption at relatively low temperatures is dominated by relaxation of the resin, significant chemical degradation occurs at 90 °C. The chemical degradation most likely involves the hydrolysis of imide units, resulting in depolymerization and chain scission. © 2002 Elsevier Science Ltd. All rights reserved.

Keywords: Water diffusion; Bismaleimide; Carbon fiber composites

1. Introduction

Thermoset resins and their composites are widely used in aerospace, automotive, civil and electronics industries due to their desirable mechanical, thermal and electrical properties. Nevertheless, one of the major disadvantages of thermoset resins is their tendency to absorb significant amounts of water when exposed to humid environments. Absorbed moisture has many detrimental effects on material performance [1–4]. Since the 1970s, tremendous efforts have been made to understand the mechanisms of moisture absorption in polymers and composites and to improve their moisture resistance.

Besides moisture, most applications also expose the material to a wide range of temperatures. As a result, the temperature effect on moisture diffusion and environmental aging is of major practical repercussion. Temperature may influence moisture absorption in polymers and composites in a complex manner.

First of all, diffusion is a thermally activated process and diffusivity is very sensitive to temperature. Diffusion coefficient obeys the activated transition state theory and its temperature dependence can be expressed by the Arrhenius

equation [4,5]

$$D = D_0 \exp\left(-\frac{E_a}{RT}\right) \quad (1)$$

in which E_a is the activation energy of diffusion, D_0 the pre-exponential factor and R is the gas constant. The exponential correlation of diffusivity with $1/T$ results in a very strong temperature dependence. Typical activation energies of moisture diffusion in thermosets range from 35 to 50 kJ/mol [6–8]. For composites with impermeable fibers, the activation energy of diffusion is expected to be the same as that of the neat resin. In reality, the activation energies of a composite and its flash are often different and such discrepancies have been used to identify the presence of highly diffusive paths or additional diffusion mechanisms in the composite [6,9,10].

Different from diffusivity, the temperature dependence of equilibrium uptake is not very well established. Many authors have reported the equilibrium moisture content to be independent of temperature [11,12], while others observed either positive or negative temperature dependences [13,14]. There is little theoretical consideration on the temperature dependence of equilibrium uptake. In contrast, the temperature effect on solubility is well established in fundamental thermodynamic theories. According to van't Hoff's equation, the temperature dependence of

* Corresponding author. Tel.: +1-734-7644312; fax: +1-734-7634788.
E-mail address: afyee@engin.umich.edu (A.F. Yee).

solubility is determined by the enthalpy change upon dissolution [14,15]

$$\frac{d \ln c_s}{dT} = \frac{\Delta H(T)}{RT^2} \quad (2)$$

In the above equation, c_s is the saturation concentration and ΔH is the heat of dissolution. In a sense, water absorption in a polymer can be treated as a dilute solution and is expected to obey van't Hoff's equation. Instead of heat of dissolution, the temperature dependence of the saturation weight gain is determined by the heat of absorption. In the narrow temperature range of normal water absorption measurements, the heat of absorption can be regarded as a constant. Hence, integrating Eq. (2) yields:

$$\begin{aligned} c_s &= c_{s,\text{ref}} \exp\left[\frac{-\Delta H_{\text{abs}}}{R} \left(\frac{1}{T} - \frac{1}{T_{\text{ref}}}\right)\right] \\ &= c_{s,\text{ref}} \exp\left[\frac{-\Delta H_{\text{abs}}}{RT}\right] \exp\left[\frac{\Delta H_{\text{abs}}}{RT_{\text{ref}}}\right] \end{aligned} \quad (3)$$

$$\text{define } c_{s0} = c_{s,\text{ref}} \exp\left[\frac{\Delta H_{\text{abs}}}{RT_{\text{ref}}}\right]$$

$$\text{then } c_s = c_0 \exp(-\Delta H_{\text{abs}}/RT)$$

$$\text{or } M_{\infty}(T) = M_0 \exp(-\Delta H_{\text{abs}}/RT)$$

in which $M_{\infty}(T)$ is the equilibrium uptake as a function of temperature, ΔH_{abs} the heat of absorption per mole of sorbed water molecules and M_0 is a temperature independent constant. According to Eq. (3), for an endothermic absorption process, the equilibrium uptake increases with temperature, while it decreases as temperature increases in an exothermic absorption.

The heat of absorption depends on interactions between the polymer and absorbent. The favorable interaction between moisture and a polar polymer may result in a negative heat of absorption. In fact, moisture absorption in epoxies has been reported to be slightly exothermic [16]. Consequently, the saturation level in epoxies is expected to decrease with increasing temperature. However, in the absence of chemical reactions between the polymer and water, the heat of moisture absorption is typically rather small. As a result, the equilibrium uptake is only weakly dependent on temperature. Within the narrow temperature range of typical moisture diffusion studies, i.e. from room temperature to 100 °C, the variation in equilibrium uptake may be difficult to determine experimentally. Moreover, diffusion is coupled with relaxation in glassy polymers and true equilibrium is often inaccessible in typical experimental timescales [4,16,17]. Consequently, the determination of equilibrium moisture uptake is a non-trivial task. This probably contributes to the contradictory results in the literature regarding to the temperature dependence of equilibrium uptake.

Besides affecting the diffusivity and equilibrium uptake, temperature may also change the fundamental diffusion

mechanism in a material. Because of the non-equilibrium characteristics of glassy polymers, moisture diffusion is coupled with the relaxation process. While the rates of diffusion and relaxation are both sensitive to temperature, their temperature dependences may be different. A change in temperature will vary the relative rates of diffusion and relaxation, thus changing the overall absorption behavior. The variation in absorption kinetics with the relative contributions of diffusion and relaxation has been theoretically derived [16,18] and experimentally observed [19,20] by several authors.

Additionally, moisture absorption at elevated temperatures may induce irreversible changes to polymers and composites, such as chemical degradation, cracking and debonding. These damages to the material will also change the weight gain behavior of the material correspondingly. For example, cracking and blistering can cause exceptionally high uptake [13,21], while the leaching of small molecule components results in gradually decreasing weight gain [22]. Furthermore, water exposure may chemically degrade the material through reactions such as hydrolysis and oxidation [23,24]. Because of the complex nature of moisture induced degradation, detailed analysis is necessary to identify the diffusion mechanisms at different temperatures.

We have reported results on moisture diffusion and hygrothermal aging in a commercial bismaleimide (BMI) resin and its composites [17,25–28]. In the current publication, the temperature effect on moisture absorption is discussed. The diffusion properties at four temperatures, i.e. 35, 50, 70 and 90 °C, are compared in an attempt to identify the environmental aging mechanisms at different temperatures. The effects of temperature on the kinetics and thermodynamics of diffusion are examined. The occurrence of chemical degradation at elevated temperature is also investigated.

2. Experimental

The BMI resin used in this research is a commercial three-component modified BMI (Cytec™ 5250-4 RTM) consisting of both BMI and diallyl components. The neat resin and composites were processed by compression molding. The resin which is a viscous liquid at room temperature was first heated to 100 °C and impregnated into the carbon fiber fabrics for 30 min. The viscosity of the resin is sufficiently low at this temperature, thus no solvent is needed for impregnation. The sample was then cured under 200 psi pressure using a step-wise curing program with 6 h at 190 °C and another 6 h at 230 °C. After curing, the glass transition temperature (T_g) of the material is 270 °C as determined by DSC and its dry density is 1.25 g/cm³.

Two types of carbon fiber fabrics are used in the composites, i.e. uni-weave and woven fabrics. Both fabrics are composed of Hexcel IM7 carbon fiber. The schematic

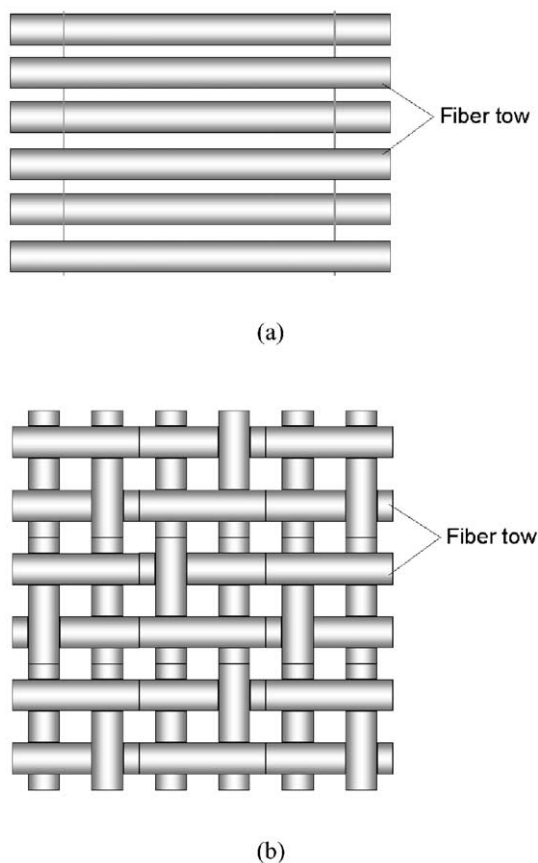


Fig. 1. Schematics of the fiber arrangement in the: (a) uni-weave fabric and (b) woven fabric.

diagrams of the fiber arrangement in the uni-weave and woven fabrics are shown in Fig. 1. In the uni-weave fabric, the majority of the fiber tows are aligned in the same direction with a very small number of transverse fibers to keep the fiber tows in place. Therefore, the uni-weave composite is essentially a unidirectional composite. The woven fabric is a 4-harness satin weave. Five composites were studied and they are uni-weave 3-ply, uni-weave 12-ply, woven 3-ply, U–W–U (uni-weave/woven/uni-weave 3-ply hybrid) and W–U–W (woven/uni-weave/woven 3-ply hybrid). During composite manufacturing, excess resin called ‘flash’ is squeezed out of the mold. Flash is ideal in comparison studies between the composite and its matrix resin since it has essentially the same thermal history as the composite. Most of the neat resin samples studied here are from the flash of different composite panels.

The moisture diffusion properties of the BMI resin and composites are determined by immersing thin sections of the material in liquid water and measuring the weight periodically. The thin specimens were obtained by cutting and polishing thicker panels. For the neat resin, the resin panels were cut and sectioned into thin specimens ($15 \times 15 \times 0.5 \text{ mm}^3$) using a low speed diamond wafering saw. To achieve uniform thickness within each specimen,

the sections were then polished using 600 grit sand paper. For the 3-ply uni-weave and woven composites, specimens of $15 \times 15 \text{ mm}^2$ were cut from the composite panels and then polished to roughly 0.5 mm in thickness. The 3-ply hybrid composite panels were cut to appropriate size without further polishing as it will change the relative content of the uni-weave and woven plies. In the case of the 12-ply uni-weave composite, diffusion along and across the fiber direction were both studied to determine the effect of interface on moisture diffusion. Diffusion specimens with the fibers parallel and perpendicular to the main surfaces were prepared by cutting the uni-weave 12-ply panel perpendicular and parallel to the fiber direction, respectively. The dimensions of these specimens are $25 \times 3.6 \times 0.5 \text{ mm}^3$. In most diffusion specimens, the thickness is much smaller than the lateral dimension. As a result, the diffusion can be regarded as a one-dimensional process. However, this assumption is no longer valid in the uni-weave 12-ply composite. Edge correction as outlined in Ref. [26] is used to correct water diffusion through the edges. The diffusivity values reported in the paper have been corrected for the edge effect when necessary.

Prior to absorption experiments, the samples were dried in a vacuum oven at about $70 \text{ }^\circ\text{C}$ until the weight stabilized. The specimens were then immersed in distilled water at different temperatures and the weight change monitored as a function of time. The absorption behavior at four different temperatures, namely, 35, 50, 70 and $90 \text{ }^\circ\text{C}$, was studied. At each temperature, at least three specimens of the same material were tested. A Perkin–Elmer AD-4 autobalance was used for the weight measurements. The activation energies of diffusion were determined by plotting the diffusivity in an Arrhenius plot.

To determine any possible chemical degradation during water absorption, the chemical composition of the resin was monitored by FT-IR. The FT-IR spectra were collected using a Nicolet Nexus 670 FT-IR spectrometer operating in the attenuated total reflection (ATR) mode. 128 scans were co-added to improve the signal-to-noise ratio. Diffusion specimens of roughly 0.5 mm thick were used directly for IR characterization without further sample preparation. During water absorption, the specimen was periodically removed from the water bath, weighed and immediately loaded into the IR spectrometer. The IR data collection lasts about 5 min and afterwards the specimen was returned to the water bath for additional absorption. To demonstrate the reversibility of any chemical changes upon desorption, the material was also characterized after drying. After prolonged water absorption, the specimen was dried in a vacuum oven at the absorption temperature until its weight stabilized. The IR spectrum was then collected and the T_g measured by DSC. A Perkin–Elmer DSC7 was used for T_g measurements. The temperature was scanned from 30 to $300 \text{ }^\circ\text{C}$ at a heating rate of $10 \text{ }^\circ\text{C}/\text{min}$.

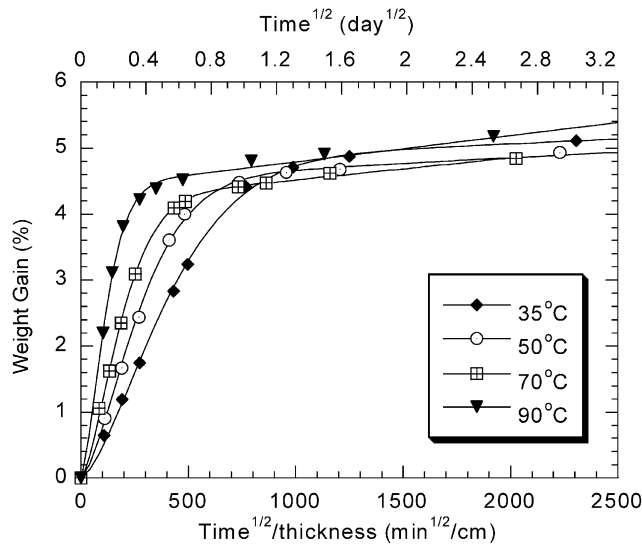


Fig. 2. Short term weight gain curves of the uni-weave 3-ply flash at various temperatures. The symbols are experimental results and the solid lines are curve fits using Eq. (4).

3. Results and discussion

3.1. Diffusivity

The typical short term absorption curves of the BMI neat resin at different temperatures are shown in Fig. 2. As expected for a thermally activated process, an increase in temperature significantly accelerates moisture diffusion. All neat resin and composites display similar two-stage diffusion behavior, which can be described by the two-stage diffusion model proposed earlier [17]. In this model, the first and second stages of moisture absorption are assumed to be diffusion- and relaxation-controlled, respectively. The mathematical form of this two-stage model is given by the following equation [17]:

$$M_t = M_{\infty 0} (1 + k\sqrt{t}) \left\{ 1 - \exp \left[-7.3 \left(\frac{Dt}{h^2} \right)^{0.75} \right] \right\} \quad (4)$$

In Eq. (4), M_t is the weight gain as a function of time, D the diffusivity, h the specimen thickness, $M_{\infty 0}$ the quasi-equilibrium uptake reached in the diffusion-controlled first stage and k characterizes the rate of relaxation during water absorption. Thus, the diffusivity can be determined by curve fitting the experimental uptake results by Eq. (4). The same procedure was followed for all neat resins and most composites except the woven 3-ply and W-U-W composites, whose weight gain curves were fitted by the dual-diffusivity model developed elsewhere [27,28]. The diffusivities at different temperatures are tabulated in Table 1. The reported diffusivity value is the average of three specimens. The relative error in the diffusivity values is estimated to be within 10% based on the reproducibility of the data among different specimens. It can be seen that a

Table 1

Diffusivities of various neat resin and composites at different temperatures

	Diffusivity (10^{-8} cm ² /s)			
	35 °C	50 °C	70 °C	90 °C
Uni-weave 3-ply flash	0.56	1.2	2.6	5.4
Uni-weave 12-ply flash	0.55	1.3	2.9	5.3
Woven 3-ply flash	0.61	1.3	2.9	–
Uni-weave 3-ply	0.30	0.67	1.3	2.9
Uni-weave 12-ply along	0.53	1.1	2.6	5.0
Uni-weave 12-ply across	0.27	0.59	1.2	2.0
Woven 3-ply ^a	0.11	0.21	0.46	–
U-W-U	0.32	0.64	1.5	2.7
W-U-W ^a	–	0.18	0.40	0.98

^a Intrinsic diffusivity in the dual-diffusivity model.

55 °C rise in temperature increases the diffusivity by nearly 10 times.

When $\ln(D)$ is plotted as a function of $1/T$ as done in Fig. 3, a linear relationship is obtained, which is consistent with the Arrhenius equation. The activation energy of the diffusion process can be calculated from the slope of the Arrhenius plot. The activation energies and pre-exponential factors of various composites and neat resins are listed in Table 2. The relative error in the activation energy and pre-exponential factor is estimated to be slightly larger than that in the diffusivity, as an additional curve fitting step is needed to determine the activation energy.

The activation energies and pre-exponential factors of the flash samples are very close to each other, which is expected as they have identical chemical composition and similar thermal histories. The activation energy of this BMI resin is also very close to the literature values of epoxies, suggesting similar diffusion mechanisms in BMI and epoxy resins. Although the chemical composition of the two resins are distinctly different, both materials are highly polar and densely crosslinked. Short term moisture diffusion in these

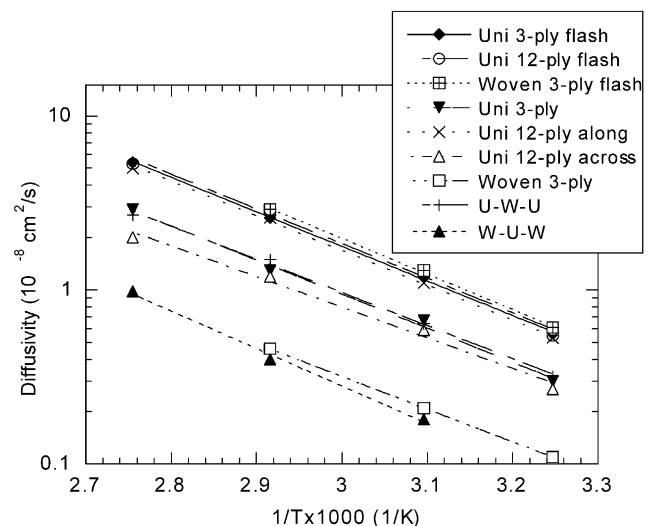


Fig. 3. Moisture diffusivity vs. $1/T$ for various neat resins and composites.

Table 2
Activation energies and pre-exponential factors of various neat resins and composites

	E_a (kJ/mol)	D_0 (10^{-2} cm ² /s)
Uni-weave 3-ply flash	38	1.6
Uni-weave 12-ply flash	38	1.7
Woven 3-ply	39	2.6
Uni-weave 3-ply	37	0.69
Uni-weave 12-ply along	38	1.58
Uni-weave 12-ply across	34	0.15
Woven 3-ply	36	0.14
U–W–U	36	0.49
W–U–W	41	0.80

two thermosets may involve very similar processes and transition states.

As for the composites, the activation energy of an ideal composite should be the same as its flash because moisture diffusion is a matrix dominated property. The presence of fiber usually only results in a changed pre-exponential factor. The observation that the activation energy in a composite is different from that of the flash usually suggests the existence of additional diffusion mechanisms such as interface- or crack-assisted diffusion. From Table 2, it can be seen that the activation energies of the composites are generally very close to those in the neat resins, while the pre-exponential factors defer from material to material, as one would expect. The largest relative difference in activation energy between the composite and neat resin is about 10%, which is estimated to be within the experimental error. The fact that similar activation energies are observed in the composites and neat resins indicates that the matrices of the composites behave very similarly to the neat resin and the effect of fiber–matrix interface on the kinetics of moisture diffusion is minimal.

It should be mentioned that diffusivity is only indicative of the diffusion mechanism during initial absorption, as the diffusion-controlled first stage reaches within quasi-equilibrium roughly one day. The absence of interface effect on diffusivity does not mean interfacial damages will not occur after prolonged environmental aging. Indeed, we have observed moisture induced interfacial cracking after extended water absorption [26,28].

3.2. Quasi-equilibrium uptake

Due to the two-stage diffusion behavior of the BMI resin and composites, the ultimate equilibrium uptake is not reached in the experimental time scale (up to 2 years). Yet, since the first and second stages of diffusion are diffusion-controlled and relaxation-controlled, respectively, the quasi-equilibrium uptake level reached at the end of the first stage corresponds to the equilibrium plateau in a Fickian diffusion. In the absorption curves shown in Fig. 2, the crossover between the first and second stages roughly corresponds to this quasi-equilibrium uptake. Quantitatively, the

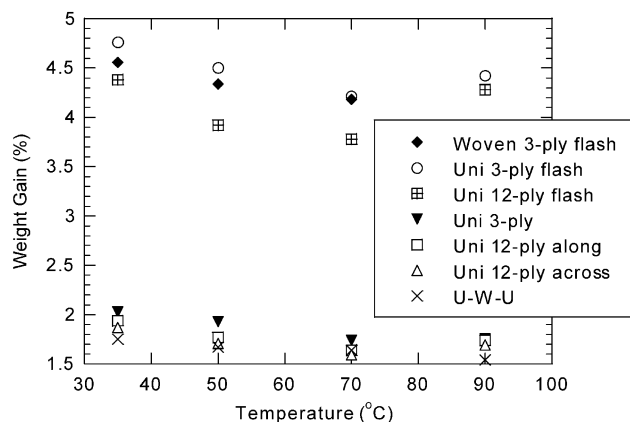


Fig. 4. Fickian equilibrium uptake ($M_{\infty 0}$) of various neat resins and composites at different temperatures.

Fickian equilibrium uptake ($M_{\infty 0}$) can be determined by curve fitting using Eq. (4). Since the quasi-equilibrium uptake represents the saturation level of a solely diffusion-controlled process, the complication caused by the coupling of diffusion and relaxation can be avoided. Hence, the temperature dependence of the Fickian equilibrium uptake can be more accurately determined.

The $M_{\infty 0}$ values of different materials determined by curve fitting are plotted in Fig. 4. The Fickian equilibrium uptake decreases with increasing temperature between 35 and 70 °C, as one would expect for an exothermic absorption process. Interestingly, it rises again at 90 °C. The reversed trend at 90 °C suggests that additional diffusion mechanisms come into play at this temperature. While moisture diffusion below 70 °C is controlled by the thermodynamics of simple diffusion, a critical temperature seems to exist between 70 and 90 °C, beyond which additional mechanisms become active during the diffusion process. The nature of the diffusion process at 90 °C will be discussed in more detail in the following sections.

Since $M_{\infty 0}$ represents the equilibrium of the diffusion controlled first stage, the equilibrium thermal dynamics relationship in Eq. (3) can be applied. According to Eq. (3), the heat of absorption can be determined from the temperature dependence of the quasi-equilibrium uptake. When $\ln(M_{\infty 0})$ is plotted as a function of $1/T$ as done in Fig. 5, the heat of absorption can be calculated from the slope of the line. Because of the changed diffusion mechanisms at 90 °C, equilibrium uptake data at 90 °C are excluded in Fig. 5. Unfortunately, as the variations in $M_{\infty 0}$ are quite small and only data at three temperatures are available, the experimental errors in ΔH_{abs} are rather high. To improve the reliability, another method based on the rate of initial absorption was also developed to calculate ΔH_{abs} .

In Fickian diffusion, the diffusivity is related to the rate of initial absorption according to the following equation:

$$D = \pi \left(\frac{h}{4M_{\infty}(T)} \right)^2 \left(\frac{dM_t}{d\sqrt{t}} \right)^2 = \pi \left(\frac{1}{4M_{\infty}(T)} \right)^2 \left(\frac{dM_t}{d\sqrt{t}/h} \right)^2 \quad (5)$$

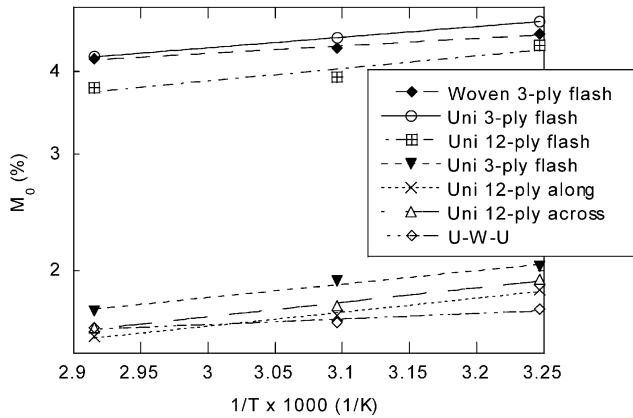


Fig. 5. Fickian equilibrium uptake vs. $1/T$ for various neat resins and composites.

In Eq. (5), $dM_t/d\sqrt{t}/h$ is the initial absorption rate, which can be easily determined from a linear fit of the initial weight gain curves as shown in Fig. 6. When D and $M_\infty(T)$ in Eq. (5) are substituted by Eqs. (1) and (3), respectively, one obtains:

$$D_0 \exp(-E_a/RT) = \pi \left(\frac{1}{4M_0 \exp(-\Delta H_{\text{abs}}/RT)} \right)^2 \left(\frac{dM_t}{d\sqrt{t}/h} \right)^2$$

$$\begin{aligned} \frac{dM_t}{d\sqrt{t}/h} &= 4M_0 \sqrt{\frac{D_0}{\pi}} \exp \left[- \left(\frac{E_a}{2} + \Delta H_{\text{abs}} \right) / RT \right] \\ &= C_0 \exp \left[- \left(\frac{E_a}{2} + \Delta H_{\text{abs}} \right) / RT \right] \end{aligned}$$

in which $C_0 = 4M_0 \sqrt{\frac{D_0}{\pi}}$ (6)

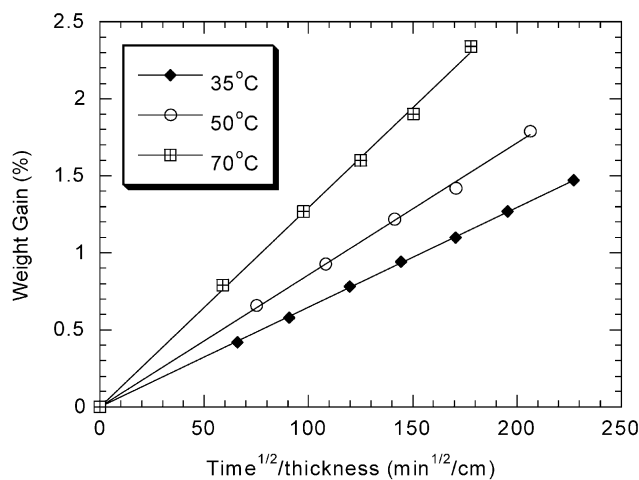


Fig. 6. Initial absorption of woven 3-ply flash at different temperatures. Solid lines are the linear curve fits that are forced to pass the origin.

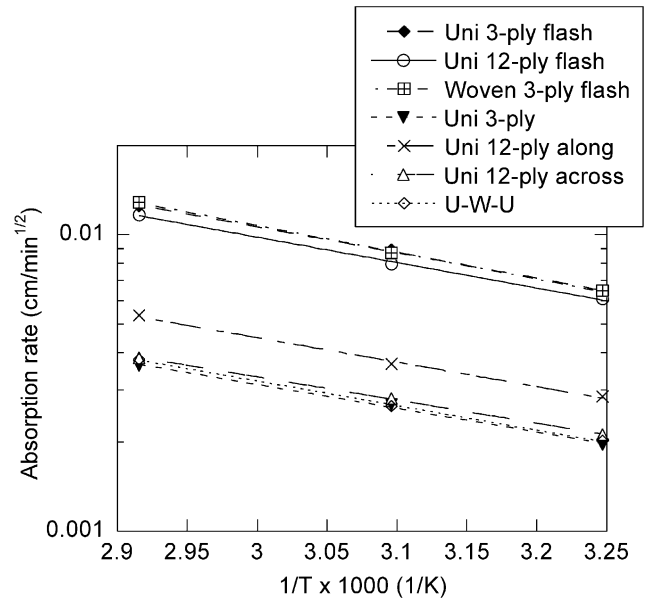


Fig. 7. Initial absorption rate vs. $1/T$ for various neat resins and composites. The lines are the exponential curve fits.

Define

$$E_r = \frac{E_a}{2} + \Delta H_{\text{abs}} \quad (7)$$

Thus

$$\ln \left(\frac{dM_t}{\sqrt{t}/h} \right) = \ln C_0 - E_r/RT \quad (8)$$

Therefore, if the initial absorption rates at different temperatures are plotted on an Arrhenius plot as done in Fig. 7, the slope is related to E_a and ΔH_{abs} by Eq. (7). Table 3 lists the ΔH_{abs} values of various materials calculated using the two methods discussed earlier.

The use of two different methods to determine ΔH_{abs} improves the reliability of the results. The average ΔH_{abs} listed in Table 3 is roughly on the order of -3 kJ/mol. The variation among different samples is considered to be within the scatter of the measurements. Similar data analysis or the direct calorimetry measurement of the heat of absorption has not been previously attempted for moisture diffusion in thermosets and composites. Therefore, no literature values of the heat of absorption are available for comparison. However, calorimetry studies on surface adsorption and water absorption by textile materials and pharmaceutical systems have been performed by many authors [29–31]. For most polymers that readily absorb water without chemically reacting with water, the integrated heat of absorption ranges from -1 to -20 kJ/mol [29,30]. For example, the integrated heat of absorption in poly-methacrylic acid hydrogel is about -1.3 kJ/mol [31], while it is roughly -5 kJ/mol in microcrystalline cellulose [30,32]. Therefore, -3 kJ/mol seems to be of the right order

Table 3
Heat of absorption of various neat resins and composites

	Method I (kJ/mol)	Method II (kJ/mol)			ΔH_{abs}^a (kJ/mol)
		E_r	E_a	$\Delta H_{\text{abs}} = E_r - E_a/2$	
Uni-weave 3-ply flash	-3.1	16.6	38.0	-2.4	-2.8
Uni-weave 12-ply flash	-3.6	16.4	38.1	-2.7	-3.2
Woven 3-ply flash	-2.2	17.3	39.1	-2.3	-2.3
Uni-weave 3-ply	-3.9	15.5	37.4	-3.2	-3.6
Uni-weave 12-ply along	-3.9	15.8	38.1	-3.3	-3.6
Uni-weave 12-ply across	-4.0	15.0	33.7	-1.9	-3.0
U-W-U	-1.6	15.9	36.4	-2.3	-2.0

^a Average of methods I and II.

of magnitude for moisture absorption by hydrophilic polymers such as BMI's.

3.3. Second-stage absorption

The long term weight gain curves of the uni-weave 3-ply flash at different temperatures are displayed in Fig. 8. As discussed previously [17], the slope of second-stage absorption is related to the rate of relaxation in the material. An increase in temperature is expected to accelerate the structural relaxation, thereby increasing the rate of absorption during the second stage of diffusion. As seen in Fig. 9, this is indeed true between 35 and 70 °C. However, the trend reverses at 90 °C, with the slope at 90 °C being unexpectedly low. Similar trends are also observed in other neat resins and composites studied in this work. The decrease in k at 90 °C implies the onset of new diffusion mechanisms at this temperature. While moisture absorption below 70 °C is dominated by the structural relaxation of the network; other processes, e.g. chemical reactions, may couple with moisture diffusion at 90 °C.

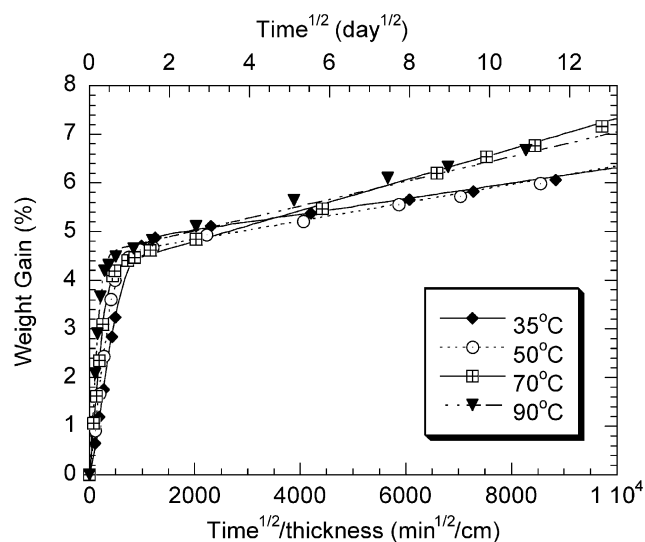


Fig. 8. Long term weight gain curves of uni-weave 3-ply flash at different temperatures. Lines are curve fits by the current two-stage model.

3.4. Chemical degradation during water absorption at elevated temperatures

The unexpected changes in Fickian plateau and k value at 90 °C suggest a change in the aging mechanism at this temperature. To identify the aging mechanism at 90 °C, FT-IR spectroscopy was performed during water absorption. Fig. 10 shows the IR spectra of the uni-weave 3-ply flash after different periods of water absorption at 90 °C. Only after 17 days at 90 °C, the intensity of the peak near 1600 cm^{-1} noticeably increased, which suggests the occurrence of chemical reactions. It seems that at 90 °C the second-stage water absorption is coupled with chemical degradation. The dramatic change in chemical structure after long term absorption at 90 °C can be clearly seen in Fig. 11, which compares the spectra of the uni-weave 3-ply flash before and after water absorption at 90 °C for 18 months. The specimen was dried before the IR measurement, therefore the chemical degradation is irreversible upon desorption. By contrast, the peak positions and relative intensities remain largely unchanged after extended

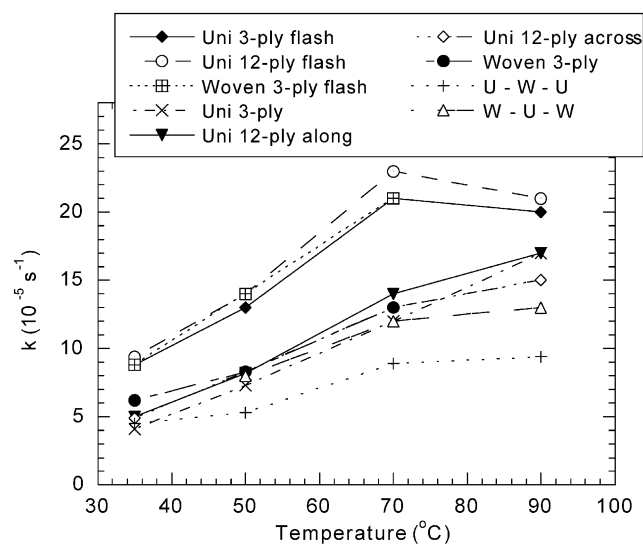


Fig. 9. Slope of the second-stage absorption of various neat resins and composites at different temperatures.

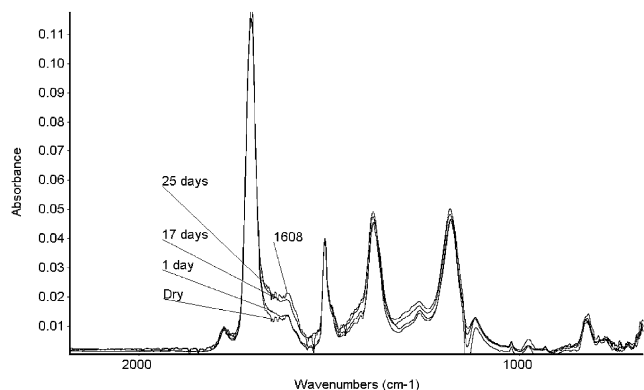


Fig. 10. Reflection IR spectra after different periods of water absorption at 90 °C.

absorption at 70 °C, as also shown in Fig. 11. The onset of considerable chemical degradation at 90 °C is probably the underlining reason for the unexpected diffusion properties discussed earlier.

Although model compounds are required to positively identify the moisture induced chemical reactions, a survey of related publications suggests that hydrolytic degradation is the most likely mechanism. Relatively little information is available on hydrolytic degradation in BMI resins; however, various studies have indicated that thermoplastic and cross-linked polyimides undergo hydrolysis under elevated temperatures and humidities [23,24,33,34]. In fact, the imidization reaction between the anhydride and amine monomers during polyimide curing is reversible, as shown in Scheme 1. The imide units can undergo ring opening reaction followed by further hydrolysis of the polyamic acids. The hydrolysis of polyamic acids results in chain scission and decrease in molecular weight.

Different from thermoplastic polyimides, the curing of BMI involves the addition polymerization and crosslinking of maleimide double bonds. As seen in Scheme 2, the same imide ring structure as those in polyimides is formed after curing. These imide units are also susceptible to hydrolytic degradation under high temperatures and humidities. Such a

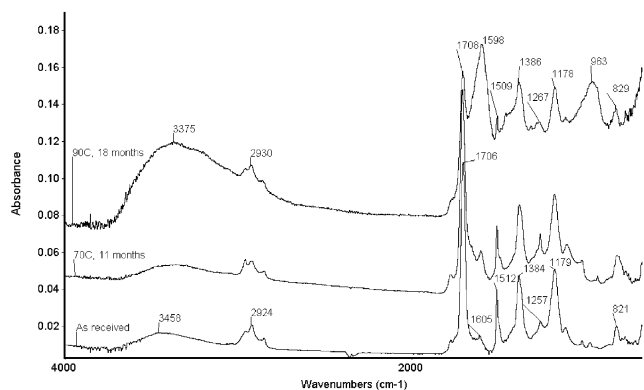
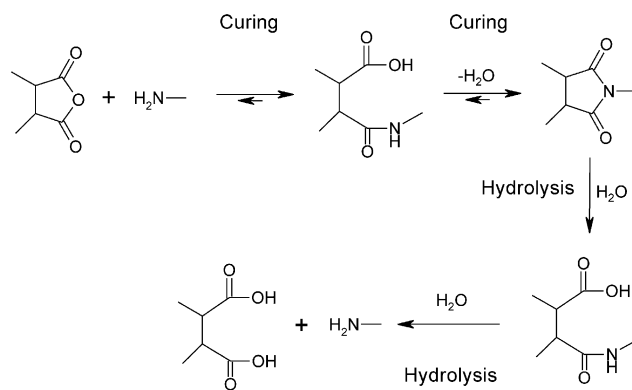
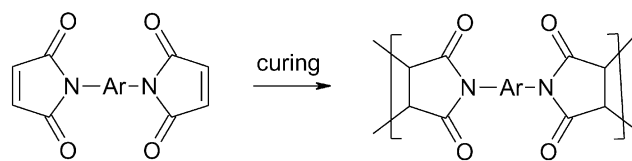


Fig. 11. FT-IR reflection spectra before and after water absorption at 70 and 90 °C. The specimens were dried before IR measurements.



Scheme 1. Curing and hydrolysis mechanisms in polyimides.



Scheme 2. Major curing reaction of BMI resins.

degradation mechanism is further supported by the significant permanent weight change after water absorption at 90 °C. When the material was dried after absorption at 90 °C for 18 months, more than 5% residual weight gain remained. As seen in Scheme 1, the complete hydrolysis of an imide ring results in the addition of two water molecules, which are chemically bonded to the structure. As a result, permanent weight increase is expected after hydrolysis. Finally, the disappearance of the glass transition temperature in the DSC scan shown in Fig. 12 also suggests significant depolymerization and chemical degradation [24].

The IR spectra in Fig. 11 can be interpreted based on the above proposed degradation mechanism and FT-IR studies on related materials in the literature [24,35–37]. For the

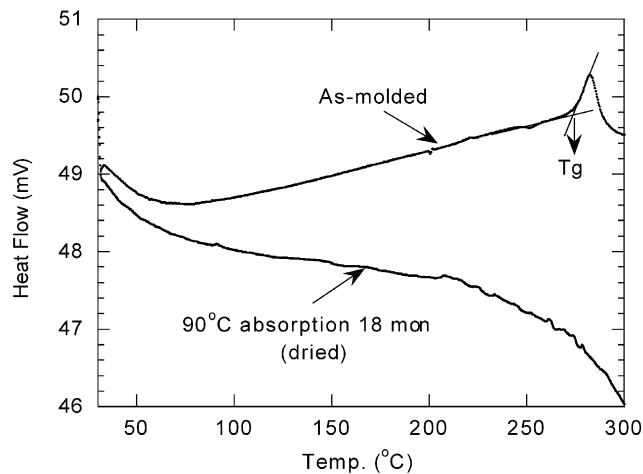


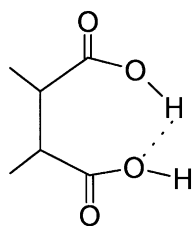
Fig. 12. DSC traces of uni-weave 3-ply flash before and after water absorption at 90 °C.

Table 4
Major peak positions and assignments in the IR spectra of BMI neat resin before and after prolonged water absorption at 90 °C

Before absorption		After absorption	
Peak position (cm ⁻¹)	Assignment	Peak position (cm ⁻¹)	Assignment
3460	O–H stretching (phenol)	3375	O–H and N–H stretching in amide and acid
1776	Characteristic imide absorption		
1706	C=O stretching	1598	N–H deformation in amide and amine
1510	Aromatic groups		
1385	C–N stretching in imide	963	Associated carboxylic acid
820	Maleimide group		

as-molded BMI resin, the assignments of major peaks are tabulated in Table 4.

After prolonged water absorption at 90 °C, the peak at 3460 cm⁻¹ moved to 3375 cm⁻¹ with dramatically increased intensity. This peak also becomes asymmetric with a long tail on the low wavenumber side, which overlaps with the C–H stretching vibration bands at around 2900 cm⁻¹. A broad O–H stretching band that overlaps with C–H stretching bands is characteristic of carboxylic acids [37]. The decreased wavenumber of this peak is also consistent with the formation of amide groups, whose N–H stretching vibration occurs between 3300 and 3100 cm⁻¹ [37]. The characteristic imide peak at 1776 cm⁻¹ decreases in intensity, which is indicative of decreased concentration of imide groups. The peak at 1706 cm⁻¹ also weakens, which may be associated with the transformation of imides into amides. Different from imides, the C=O stretching band of secondary amides appears in the range 1680–1630 cm⁻¹. A very strong and asymmetric peak emerges at 1598 cm⁻¹ after water absorption. This peak is probably due to the combination of the N–H deformation band in amines and the so-called amide II band, which is associated with the combined motion of N–H bending and C–N stretching [37]. Finally, a broad peak at 963 cm⁻¹ appears after water absorption. This peak is characteristic of self-associated carboxylic acid in the presence of hydrogen bonding. Because of the close proximity between the two carboxylic groups in the diacids formed by hydrolysis, intra-molecular hydrogen bonding is very likely (Scheme 3). The resulting O–H···O out of plane deformation appears near 960 cm⁻¹ [36]. From the discussion made earlier, it can be seen that



Scheme 3. Intra-molecular hydrogen bonding in the diacid formed after imide hydrolysis.

the major changes in the IR spectrum after water absorption at 90 °C can all be accounted for by the imide ring hydrolysis mechanism shown in Scheme 1. Although a very small amount of other reactions such as oxidation may also occur during absorption, they are probably negligible and beyond the sensitivity of IR spectroscopy.

The discussion made earlier indicates that chemical degradation is coupled with structural relaxation in the second stage of water absorption. The unexpected weight gain behavior at 90 °C can be explained by the onset of such a degradation mechanism at this or a slightly lower temperature. The hydrolysis of imide groups is likely an endothermic reaction. When moisture diffusion and hydrolysis occur simultaneously, the overall heat of absorption may also become positive. Based on the thermodynamic argument, the equilibrium uptake would increase with temperature for an endothermic absorption process. This might be the reason why the quasi-equilibrium uptake increases from 70 to 90 °C. Furthermore, since a significant fraction of water molecules chemically react with the resin as suggested by the IR results, these water molecules do not effectively plasticize the resin. As a result, the relaxation rate is decreased at 90 °C, causing lower absorption rate during the second-stage diffusion.

The change of diffusion mechanism at elevated temperatures has important implications on accelerated testing. Most polymers and composites are intended for long term use and their lifetime prediction is an important design parameter. However, because of the formidable amounts of time required by tests under normal ambient conditions, such long term absorption testing is usually not viable. Consequently, accelerated aging tests are often necessary. The most commonly used method of acceleration is by increasing the diffusion temperature because of the Arrhenius correlation between diffusivity and temperature. The accelerated testing results are then extrapolated back to the service temperature to predict the long term durability of the material. However, such accelerated tests are only justified if the absorption and degradation mechanisms at the elevated testing temperature remain the same as those under the actual service conditions [38–40].

The change in degradation mechanism between 70 and

90 °C raises questions about the validity of accelerated testing achieved exclusively by elevating the temperature. The absorption data acquired at an elevated temperature cannot be simply extrapolated to lower temperatures to predict the long term performance of the material. Instead, reliable environmental resistance data need to be obtained by testing under realistic ambient conditions.

4. Conclusions

Moisture diffusion behaviors of the BMI resin and various composites at four different temperatures, i.e. 35, 50, 70 and 90 °C, are compared and analyzed. Temperature affects moisture absorption in several aspects. First, as diffusion is a thermally activated process, an increase in temperature accelerates short term diffusion and increases the diffusion coefficient. The activation energy of diffusion is close to the literature values of moisture diffusion in epoxies. The activation energy of the composites is also very close to that of the neat resin, indicating minimal interface effect on the kinetics of diffusion. Secondly, as moisture absorption by BMI is an exothermic process, the quasi-equilibrium uptake of the first-stage diffusion decreases with temperature. The heat of absorption was calculated using the quasi-equilibrium data at different temperatures. Finally, changes in temperature may also alter the degradation mechanism during water absorption. Although structural relaxation dominates moisture absorption at temperatures below 70 °C, considerable chemical degradation occurs during water absorption at 90 °C. The chemical degradation primarily involves the hydrolysis of polyimide rings, which eventually leads to chain scission and permanent weight increase. The change in the degradation mechanism between 70 and 90 °C emphasizes the need for a complete understanding of the absorption behaviors at different temperatures before accelerated testing programs can be reliably designed.

Acknowledgements

The authors want to thank Prof. Hung-Jue Sue's research group at Texas A & M University for providing all the materials and valuable discussions. This research is funded by US Air Force Office of Scientific Research (AFOSR), Grant No. F-49620-98-1-0377 and supplemented by a grant from the Institute of Materials Research and Engineering (IMRE) of Singapore. The valuable comments and suggestions of Dr Charles Y.-C. Lee in AFOSR and Prof. Roger J. Morgan in Texas A & M University are highly appreciated.

References

[1] Komorowski JP. National Aeronautical Establishment. National Research Council of Canada, Aeronautical Note NAE-AN-12, NRC No. 21300; 1983.

[2] Komorowski JP. National Aeronautical Establishment. National Research Council of Canada, Aeronautical Note NAE-AN-11, NRC No. 21299; 1983.

[3] Komorowski JP. National Aeronautical Establishment. National Research Council of Canada, Aeronautical Note NAE-AN-10, NRC No. 22700; 1983.

[4] Weitsman Y. Comprehensive composite materials. In: Talreja R, Manson J-AE, editors. Polymer matrix composites, vol. 2. New York: Elsevier, 2000.

[5] Komorowski JP. National Aeronautical Establishment. National Research Council of Canada, Aeronautical Note NAE-AN-4, NRC No. 20974; 1983.

[6] Loos AC, Springer GS. *J Compos Mater* 1979;13:131–47.

[7] DeLasi R, Whiteside JB. Advanced composite materials-environmental effects, ASTM STP 658. American Society for Testing and Materials, 1978. p. 2–20.

[8] Long ERJ. NASA Technical Paper 1474; 1979.

[9] Whitney JM, Browning CE. Advanced composite materials-environmental effects, ASTM STP 658. American Society for Testing and Materials, 1978. p. 43–60.

[10] Blikstad M. Environmental effects on composite materials. Technomic Publishing Company, 1988.

[11] McKague EL, Reynolds JD, Halkias JE. *J Engng Mater Technol* 1976;92–5.

[12] Chateauminis A, Vincent L, Chabert B, Soulier JP. *Polymer* 1994;35:4766–79.

[13] Chaplin A, Hamerton I, Herman H, Mudhar AK, Shaw SJ. *Polymer* 2000;41:3945–56.

[14] El-Sa'ad L, Darby MI, Yates B. *J Mater Sci* 1990;25:3577–82.

[15] Sandler SI. Chemical and engineering thermodynamics. 3rd ed. New York: Wiley, 1999.

[16] Apicella A. In: Lee SM, editor. Encyclopedia of composites, Weinheim: VCH, 1990.

[17] Bao L-R, Yee AF, Lee CY-C. *Polymer* 2001;42:7327–33.

[18] Berens AR, Hopfenberg HB. *Polymer* 1978;19:489–96.

[19] Berens AR. *Polymer* 1977;18:697–704.

[20] Mijovic J, Weinstein SA. *Polym Commun* 1985;26:237–9.

[21] Burcham LJ, Vanlandingham MR, Eduljee RF, Gillespie JW. *Polym Compos* 1996;17:682–90.

[22] Zhou JM, Lucas JP. *Compos Sci Technol* 1995;53:57–64.

[23] Morgan RJ, Shin EE, Lincoln JE, Zhou JM, Drzal LT, Wilenski MS, Lee A, Curliss D. Proceedings of the 43rd International SAMPE Symposium. Society for the Advancement of Material and Process Engineering; 1998. p. 106–19.

[24] Shin EE, Morgan RJ, Zhou J. Proceedings of the 44th International SAMPE Symposium. Society for the Advancement of Material and Process Engineering; 2000. p. 389–401.

[25] Bao L-R, Yee AF. *Polym Mater Sci Engng* 2001;85:495–6.

[26] Bao L-R, Yee AF. Submitted for publication; 2002.

[27] Bao L-R, Yee AF. Submitted for publication; 2002.

[28] Bao L-R, Yee AF. Submitted for publication; 2002.

[29] Della Gatta G. *Thermochim Acta* 1985;96:349–63.

[30] Markova N, Sparr E, Wadso L. *Thermochim Acta* 2001;374:93–104.

[31] Bouwstra JA, Salomons-de Vries MA, Van Miltenburg JC. *Thermochim Acta* 1995;248:319–27.

[32] Hollenbeck RG, Peck GE, Kildsig DO. *J Pharm Sci* 1978;67:1599–606.

[33] Pryde CA. ACS symposium series 407. American Chemical Society, 1988 pp. 57–66.

[34] Murphy PD, Di Pietro RA, Lund CJ, Weber WD. *Macromolecules* 1994;27:279–86.

[35] Morgan RJ, Shin EE, Rosenberg B, Jurek A. *Polymer* 1996;38:639–46.

[36] Roeges NPG. A guide to the complete interpretation of infrared spectra of organic structures. New York: Wiley, 1994.

[37] Socrates G. Infrared characteristic group frequencies. New York: Wiley, 1980.

- [38] Martin R, Campion R. *Mater World* 1996;4:200–2.
- [39] Choqueuse D, Davies P, Mazeas F, Baizeau R. In: Gates TS, Zureick A-H, editors. *High temperature and environmental effects on polymeric composites*, vol. 2. American Society for Testing and Materials, 1997.
- [40] Prian L, Pollard R, Shan R, Mastropietro CW, Gentry TR, Bank LC, Barkatt A. In: Gates TS, Zureick A-H, editors. *High temperature and environmental effects on polymeric composite*, vol. 2. American Society for Testing and Materials, 1997.